Int. J. Electrochem. Sci., 15 **(2020)** 1450 – 1464, doi: 10.20964/2020.02.28

International Journal of
ELECTROCHEMICAL
SCIENCE
www.electrochemsci.org

Preparation and Corrosion Resistance of AKT-Waterborne Polyurethane Coating

Xia Wang[*], *Li Hou, Ling-long Xu, Xiong Li, Huan Jiang, Wen-jie Zhou*

School of Material Science and Engineering, Southwest Petroleum University, Chengdu 610500, People's Republic of China
[*]E-mail:hli0825@163.com

Received: 30 September 2019 / *Accepted:* 19 November 2019 / *Published:* 31 December 2019

In this paper, an inorganic-organic composite modification of nano-TiO_2 has been carried out using aluminum sulfate octahydrate and γ-aminopropyltriethoxysilane (KH550) to obtain AKT with good dispersion performance. The AKT-WPU composite coating with different amounts of nano-TiO_2 added was prepared by blending AKT with waterborne polyurethane (WPU). The nano-TiO_2, before and after modification, was analyzed by Fourier transform infrared spectroscopy and indicates that alumina and KH550 can be successfully grafted onto the surface of nano-TiO_2. Our thermogravimetric analysis shows that the heat resistance of the AKT-WPU composite coating was improved. The corrosion resistance of the AKT-WPU composite coatings was investigated by electrochemical impedance spectroscopy and polarization curves. Our results show that the addition of AKT significantly improves the corrosion resistance of the composite coating. The resistive modulus of the composite coating with 0.7% AKT addition amounted to 5.05×10^6 Ω. The corrosion current density is 5.21×10^{-9} A, which is more than two orders of magnitude lower than that with the pure WPU coating. The corrosion inhibition efficiency can reach 99.54%. The coating was subjected to a long-term immersion test and observed by a scanning electron microscope. After immersion for 360 h, our results show that the coating still protected the stainless steel.

Keywords: nano-TiO_2; waterborne polyurethane; corrosion resistance

1. INTRODUCTION

Environmental awareness has grown rapidly over the past decades. Therefore, water-based polyurethane (WPU) coatings have become increasingly favored as "environmentally friendly" processes and procedures all along the value chains throughout the world[1]. A WPU coating uses water as a dispersing agent and has the following characteristics: low price, non-toxic, non-polluting, easy to store, and wear resistant[2~4]. However, when hydrophilic groups are introduced into the waterborne polyurethane molecule, it results in poor water resistance and corrosion resistance, which limits the

application range of WPU in the field of anticorrosion[5~7]. To solve this problem, researchers have used nanoparticles as fillers to enhance the water resistance and corrosion resistance of WPU coatings. In recent years, the use of nano-TiO_2 as a filler to enhance the water resistance and corrosion resistance of WPU coatings has generated considerable discussion. Nano-TiO_2 is widely used in the field of coatings because it has UV protection, weather resistance, and chemical inertness[8~10]. Cui[11] added nano-TiO_2 to the polydimethylsiloxane (PDMS) matrix, and prepared a nanocomposite coating on the surface of the aluminum alloy by spin coating, thereby improving the corrosion resistance of the metal. However, the surface of the nano-TiO_2 particles has extremely strong activity, small particle size, and high surface energy. Therefore, it is difficult to disperse evenly in waterborne coatings, which seriously affects the performance and service life of its application[12]. Wang[13] studied the effect of graft modification of silane coupling agents on the dispersibility of nano-TiO_2. The results of this research show that the modified nano-TiO_2 has low surface energy and good dispersion in solvents. Studies have shown that nano-TiO_2 can reduce surface activity and weaken self-agglomeration after inorganic surface modification[14], and that organic modification can reduce the surface tension of nano-TiO_2 and enhance the dispersion stability of nano-TiO_2 in a polymer matrix[15]. Modification of nano-TiO_2 to enhance the dispersion and stability of nanoparticles in waterborne coatings is key to enhancing the anti-corrosion performance of WPU coatings[16~18].

In this study, the inorganic-organic composite modification of nano-TiO_2 is carried out through the use of aluminum sulfate octahydrate and the silane coupling agent KH550 to obtain AKT nanoparticles with good dispersion performance. A AKT-WPU composite coating with different nano-TiO_2 addition amounts was prepared by blending AKT, as a filler, with WPU. The water resistance, heat resistance, and corrosion resistance of the AKT-WPU composite coatings are investigated.

2. EXPERIMENT

2.1 Materials

Rutile nano TiO_2 was provided by the Shanghai Aladdin Biochemical Technology Co., Ltd. Waterborne polyurethane was provided by the Shenzhen Yoshida Chemical Co., Ltd. Aluminum sulfate and the silane coupling agent KH550 as well as the anhydrous ethanol and ammonia used in this paper were provided by the Chengdu Kelon Chemical Reagent Factory.

2.2 Modification of nanometer TiO_2

Our preparation began by taking 3 g of nano-TiO_2 and mixing it well with an appropriate amount of sodium hexametaphosphate in 100 mL of deionized water. We then conducted ultrasonic dispersion for 30 min, adjusted the pH of 9, stired at 80°C and slowly added a certain concentration of aluminum sulfate solution. The reaction was carried out for 4 h, aged and washed, and then dried at 110°C for 24 h to obtain AT.

Next, 2 g of AT was added to a mixture of absolute ethanol and deionized water in a volume ratio of 1:1, adjusting the pH of 9. A solution of KH550 in ethanol was slowly added dropwise at 80°C,

and the reaction was stirred rapidly for 2 h. The obtained precipitate was washed with ethanol and deionized water, and then dried at 80°C for 24 h to obtain the inorganic-organic composite modified nano TiO_2 (AKT).

2.3 Preparation of the AKT-WPU composite coating

The AKT was added to the aqueous polyurethane in a certain ratio (the mass fraction of the AKT was 0%, 0.3%, 0.5%, 0.7%, 0.9%, 1.2%, and 1.5%), and subjected to ultrasonic stirring for 30 min. The AKT-WPU composite emulsion was obtained after mechanical stirring for 1 h. The composite emulsion was then applied to the surface of the pretreated 304 stainless steel using a linear applicator, and the coating was cured at 60°C for 24 h, the thickness of the coating was (80±5) μm.

2.4 Characterization

Fourier transform infrared spectroscopy (FTIR) analysis of nano-TiO_2 particles before and after modification was carried out using the Nicolet 6700. The spectrum was recorded in the wavenumber range of 500~4000 cm^{-1} using KBr powder.

The DSC823 TGA/SDTA85/e instrument was used to analyze the thermal stability of the coating from 40°C to 600°C at a heating rate of 10°C/min under a nitrogen atmosphere.

The contact angle was measured by using a micro-syringe, at room temperature, to obtain a static contact angle from 5 μl of water droplets on the surface of the coating by a contact angle goniometer (JGW-360A).

Impedance spectra and polarization curves were recorded using a CS310 electrochemical workstation. The electrochemical test uses a conventional three-electrode system with a platinum electrode as the auxiliary electrode, a saturated calomel electrode as the reference electrode, and a coated 304 stainless steel sample as the working electrode. First, an electrochemical impedance test was performed with a scanning frequency range of 10^{-5}~10^{-2} Hz and an amplitude of 20 mV. Then, a potential dynamics scan was performed at a scan speed of 0.5 mV/s in a scan range of -0.7 V to 0.7 V (relative to the open circuit potential). According to the polarization resistance value, the corrosion inhibition efficiency (η) is calculated by the following equation:

$$\eta(\%) = \frac{R_p - R_{p0}}{R_p} \times 100\% \quad (1)$$

where R_p is the polarization resistance of the AKT-WPU coating, and R_{p0} is the polarization resistance of the bare steel.

A ZEISS EV0 MA15 scanning electron microscope (SEM) was used to analyze and observe the surface corrosion morphology of the AKT-WPU composite coating after soaking it in a 3.5% NaCl solution. The image magnification was 5 kX and the acceleration voltage was 20 kV.

3. RESULTS AND DISCUSSION

3.1 Characterization of AKT

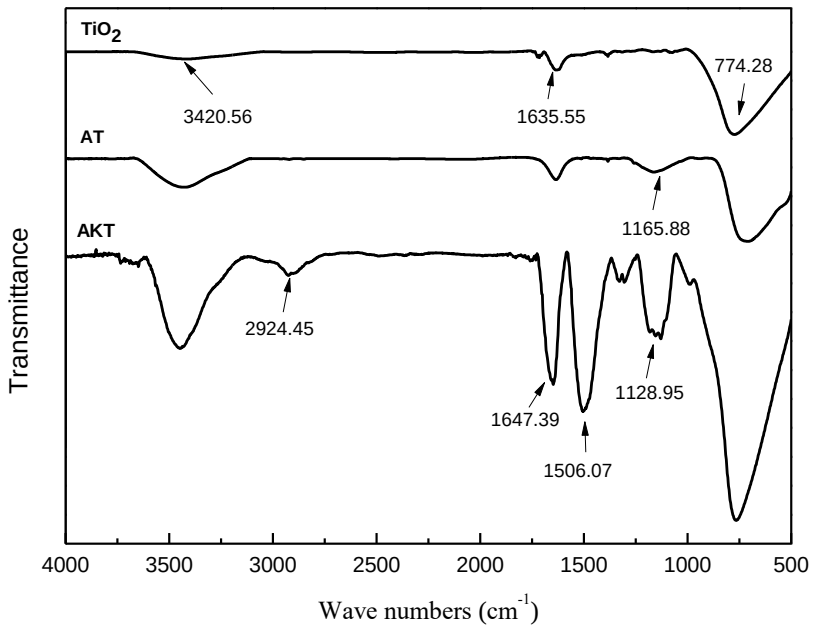

Figure 1. FTIR spectrum of nano-TiO_2 before and after modification

Fig. 1 shows, that the -OH peak, appearing at 3,420.56 cm^{-1}, adsorbed the hydroxyl groups on the surface of the TiO_2. The Ti-O-Ti bond at 774.28 cm^{-1} has a characteristic absorption peak of TiO_2. The new absorption peak of AT, at 1,165.88 cm^{-1}, is caused by the stretching vibration of Al-O-Al, indicating that the surface of the nano-TiO_2 is coated with alumina. The peak of the AKT line, at 3,446.77 cm^{-1}, is sharper than that before the modification, indicating that the hydroxyl group on the surface of the nano-TiO_2 is not completely involved in the reaction but rather, is due to the steric hindrance effect, resulting in intermolecular bonded hydrogen bonds. The absorption peak, appearing at 2,924.45 cm^{-1}, is the C-H stretching vibration peak in the modified group -CH_2. The N-H bending vibration absorption peak appears at 1,506.07 cm^{-1}, and the antisymmetric stretching vibration peak of the Si-O-Si and the stretching vibration peak of inorganic modified Al-OH-Al appear at 1,128.95 cm^{-1}[19]. The infrared spectroscopy indicated that the silane coupling agent KH550 was successfully grafted onto the surface of the nano-TiO_2, and that the inorganic-organic composite modification of the nano-TiO_2 was successful.

3.2 Water resistance of the AKT-WPU composite coating

Water absorption and hydrophobicity are important indicators for evaluating the water resistance of a coating[20,21]. The lower the water absorption of the anti-corrosion coating or the greater the water contact angle, the better the water resistance of the coating. We analyzed the water absorption properties

of different contents of the AKT-WPU composite coatings by the immersion weighing method. The water absorption of the AKT-WPU coating was calculated by the following equation:

$$W = \frac{w_2 - w_1}{w_1} \times 100\% \quad (2)$$

where W_1 is the initial mass of the coating and W_2 is the mass after soaking it for 48 h in a 3.5% NaCl solution.

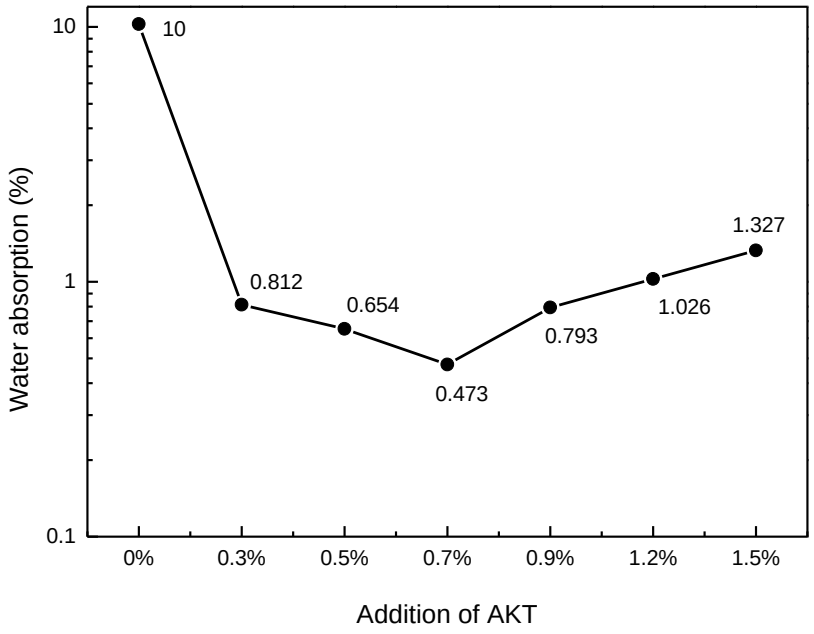

Figure 2. Effect of AKT Addition on Water Absorption Rate of AKT-WPU Coating

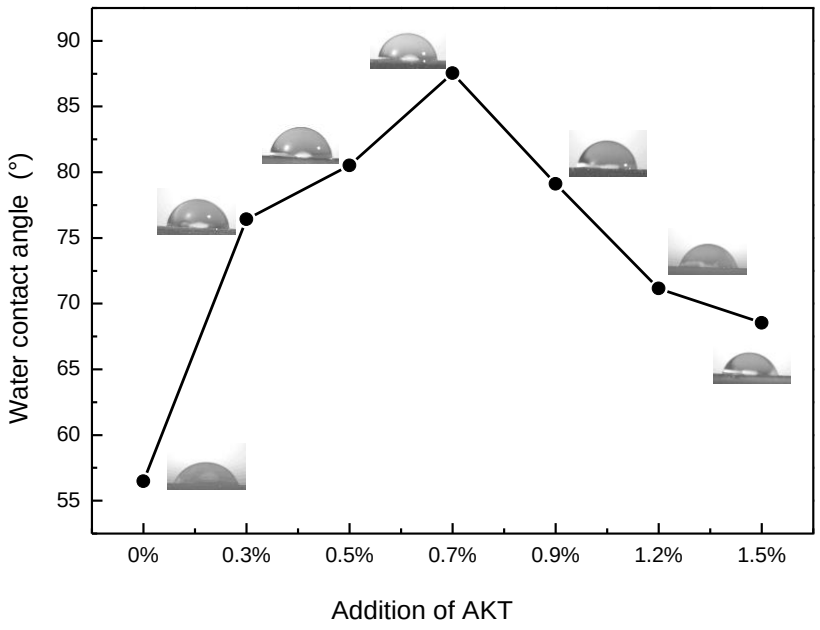

Figure 3. Effect of AKT Addition on Hydrophobicity of AKT-WPU Coating

Our results indicate that the water absorption of the coating is an important cause of poor coating protection, which will reduce the adhesion of the coating. Therefore, reducing the water absorption of the coating can improve the protective properties of the coating. As shown in Fig. 2 and Fig. 3, compared with the pure WPU coating, the water absorption of the AKT-WPU composite coating is significantly reduced, and the water contact angle is significantly increased. Because AKT is nanoparticle in size, it can be filled into the gap of the aqueous polyurethane emulsion, thus hindering the entry of corrosive ions. As the amount of AKT added increases, the water absorption of the coating first increases and then decreases, because a small amount of nanoparticles can make the void filling incomplete and cause some corrosive ions to enter the matrix. At the same time, excess AKT causes agglomeration, which is unevenly dispersed in the aqueous polyurethane emulsion, thereby forming larger voids and accelerating the corrosion of corrosive ions to the substrate[22]. The coating with 0.7% AKT added has a water absorption of at least 0.47% and a water contact angle that increased from 57.68° to 86.51°. At this time, the water resistance of the coating is optimal. Xu[23] tested the water absorption and contact angle of modified WPU film in the same way; their, results were similar to those found in this paper.

3.3 Heat resistance of the AKT-WPU composite coating

The results of our comparative thermogravimetric analysis of the pure WPU coating and the AKT-WPU composite coating are shown in Fig. 4. The pure WPU coating had an initial pyrolysis temperature of 240°C and a termination temperature of 432°C. The initial pyrolysis temperature of the AKT-WPU composite coating was 255°C and the termination temperature was 447°C. The weight loss rate of the pure WPU coating and the AKT-WPU composite coating reached 5% at 280°C and 302°C, and the final residual amounts were 5.1% and 7.9%, respectively.

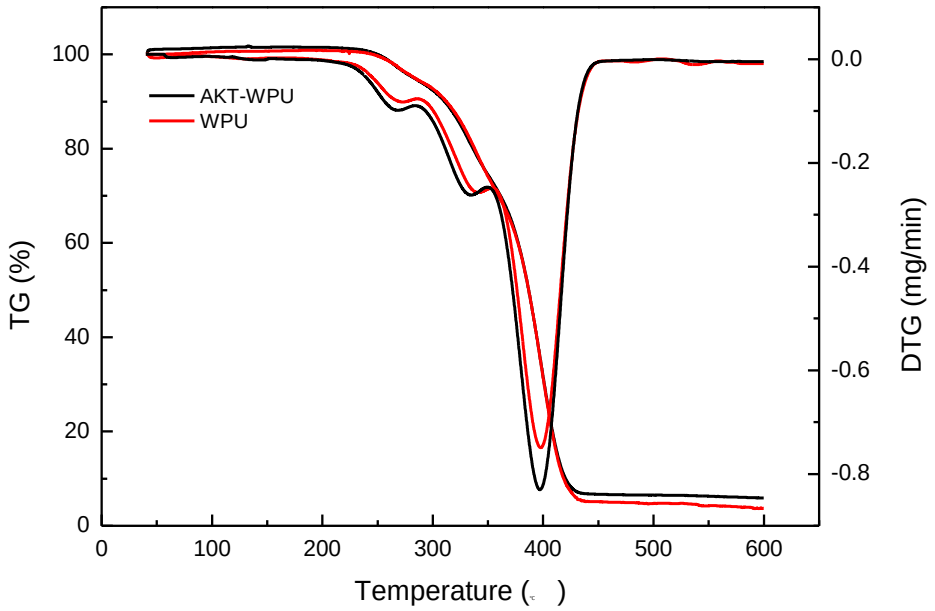

Figure 4. TGA curves of WPU coatings and AKT-WPU coatings

The decomposition temperature of the modified composite coating was increased by 15°C, and the decomposition rate was reduced by 2.8%. These results indicate that the thermal stability of the composite coating is improved after the addition of AKT particles. Deng[24] filled WPU with nano-TiO_2 modified by dopamine (DA). The thermal properties of the WPU/DA-TiO_2 films, when compared with pure WPU, were also improved.

3.4 Corrosion resistance of AKT-WPU composite coating

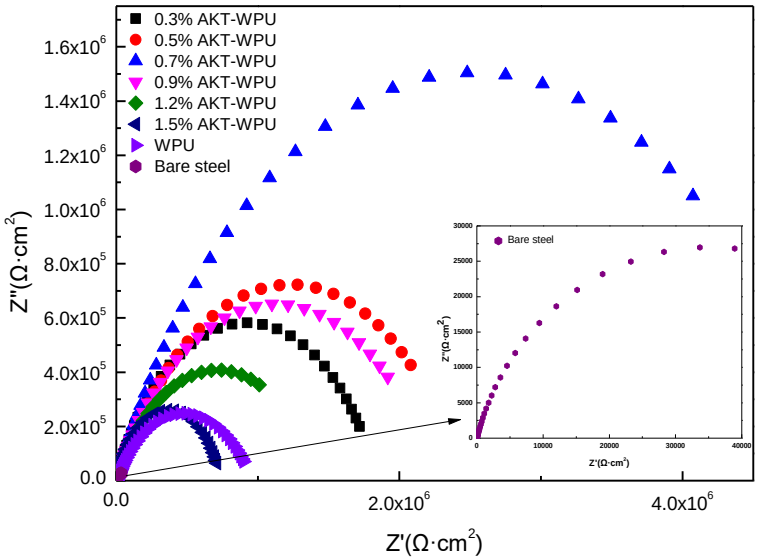

Figure 5. (a) Nyquist plots of different AKT content coatings after immersion in 3.5%NaCl solution for 12h

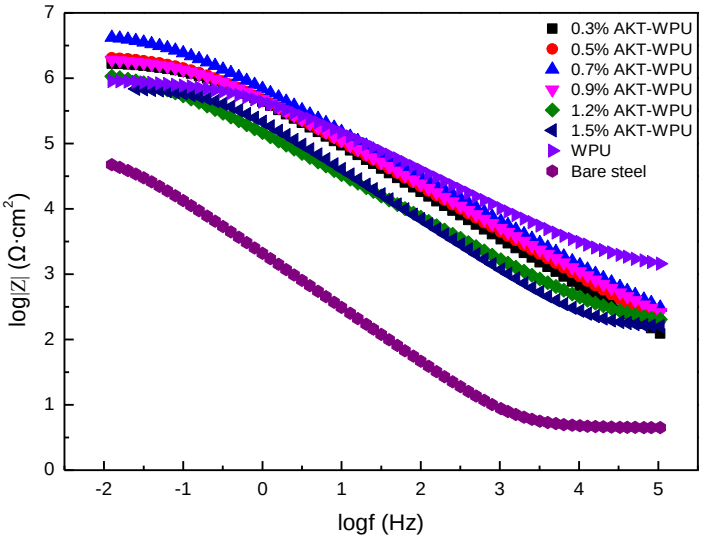

Figure 5. (b) Bode plots of different AKT content coatings after immersion in 3.5%NaCl solution for 12h

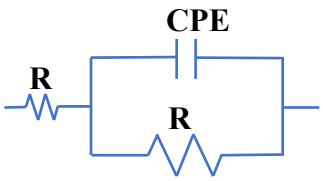

Figure 6. Equivalent circuit diagram of AKT-WPU

In order to determine the effect of the various added amounts of AKT on the corrosion resistance of the coating, different addition amounts of the AKT-WPU composite coating were prepared. The Electro Interstitial Scanning (EIS) measurement was carried out after immersing it in a 3.5% NaCl solution for 12 h, and the impedance spectrum is shown in Fig. 5.

Table 1. Data of Rs and Rc for different AKT content coatings by Nyquist plots fitting.

Sample	Rs (Ω)	CPE (F)	Rc (Ω)
Bare steel	34.46	1.03×10^{-4}	7.05×10^{4}
WPU	41.61	5.00×10^{-6}	9.57×10^{5}
0.3%AKT-WPU	61.01	7.35×10^{-7}	1.79×10^{6}
0.5%AKT-WPU	67.42	5.30×10^{-7}	2.11×10^{6}
0.7%AKT-WPU	69.11	3.82×10^{-7}	5.05×10^{6}
0.9%AKT-WPU	56.54	4.86×10^{-7}	2.08×10^{6}
1.2%AKT-WPU	54.17	1.91×10^{-6}	1.43×10^{6}
1.5%AKT-WPU	48.15	9.67×10^{-7}	7.40×10^{5}

Fig. 5(a) shows that, the impedance arc of the AKT-WPU composite coating is significantly improved compared to the impedance spectrum of the pure WPU coating. This result indicates that the addition of AKT effectively improves the corrosion resistance of the coating. The impedance arc of the AKT-WPU composite coating increases first and then decreases with an increase in the amount of AKT added. Because the addition of AKT nanoparticles can reduce the pores and gaps inside the coating and improve the compactness of the coating, thereby improving its corrosion resistance. The coating with 0.7% AKT added has the largest impedance arc. However, the addition of excess amounts of AKT causes agglomeration between the particles, thereby re-forming voids in the coating and reducing the corrosion resistance of the coating. When the amount added reaches 1.5%, the impedance arc of the composite coating is even smaller than that of the pure WPU coating. This is because the agglomeration of the excess AKT particles causes the coating voids to become large, and the coating structure is loose, which provides a channel for the electrolyte solution to penetrate into the coating and causes corrosion. It can also be seen from Fig. 5(b) that when 0.7% AKT is added, log(z)~log(f) is a diagonal with a slope of 1 indicating that the coating at this time is equivalent to a barrier layer with large resistance and small

capacitance. According to the equivalent circuit model shown in Fig. 6, the impedance data are fitted, and the impedance fitting parameters are obtained as shown in Table 1. Rs represents the solution resistance. The solution used in this experiment was consistent and the difference between the solution resistance and the coating resistance was large and negligible. Here Rc represents the coating resistance, reflecting the ability of the coating to block the electrolyte, which is the main parameter for evaluating the corrosion resistance of the coating. The coating resistivity of 0.7% AKT is as high as 5.05×10^{6} Ω, and the capacitance of the coating is 3.82×10^{-7} F. The coating has the best corrosion resistance. The same EIS test shows that the corrosion resistance of WPU coatings can be improved by adding nano-fillers. Jing[25] used hydroxylated hexagonal boron nitride (BN) nanosheets as reinforcement materials for the WPU based composite coatings, effectively improving corrosion resistance and prolonging the durability of the coatings. These experimental results show that its corrosion resistance is similar to that presented in this paper.

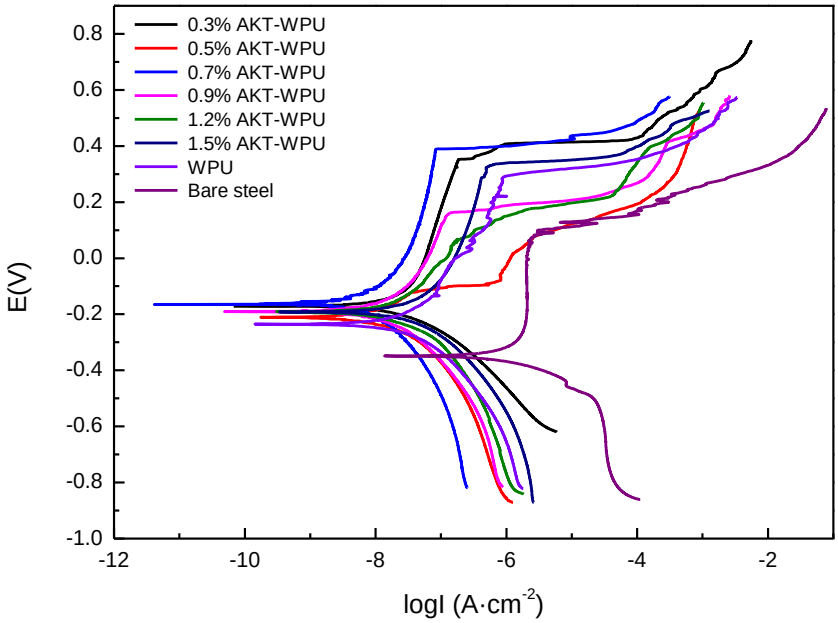

Figure 7. Polarization curves of different AKT content coatings after immersion in 3.5%NaCl solution for 12h

Table 2. Data of corrosion potential, corrosion current with corrosion rate for different AKT content coatings by polarization curve fitting

Sample	$-E_{corr}$ (V)	I_{corr} (A)	Corrosion rate (mm/year)	polarization resistance (Ω)	η (%)
Bare steel	0.350	1.12×10^{-6}	1.32×10^{-2}	2.32×10^{4}	—
WPU	0.265	2.82×10^{-7}	3.40×10^{-3}	1.28×10^{6}	98.19
0.3%AKT-WPU	0.202	1.72×10^{-8}	2.03×10^{-4}	1.51×10^{6}	98.47
0.5%AKT-WPU	0.211	9.86×10^{-9}	1.16×10^{-4}	2.65×10^{6}	99.12

0.7%AKT-WPU	0.162	5.20×10^{-9}	6.13×10^{-5}	5.01×10^{6}	99.54
0.9%AKT-WPU	0.190	9.17×10^{-9}	1.08×10^{-4}	2.84×10^{6}	99.18
1.2%AKT-WPU	0.191	1.46×10^{-8}	1.72×10^{-4}	1.79×10^{6}	98.70
1.5%AKT-WPU	0.192	2.58×10^{-8}	3.03×10^{-4}	1.01×10^{6}	97.71

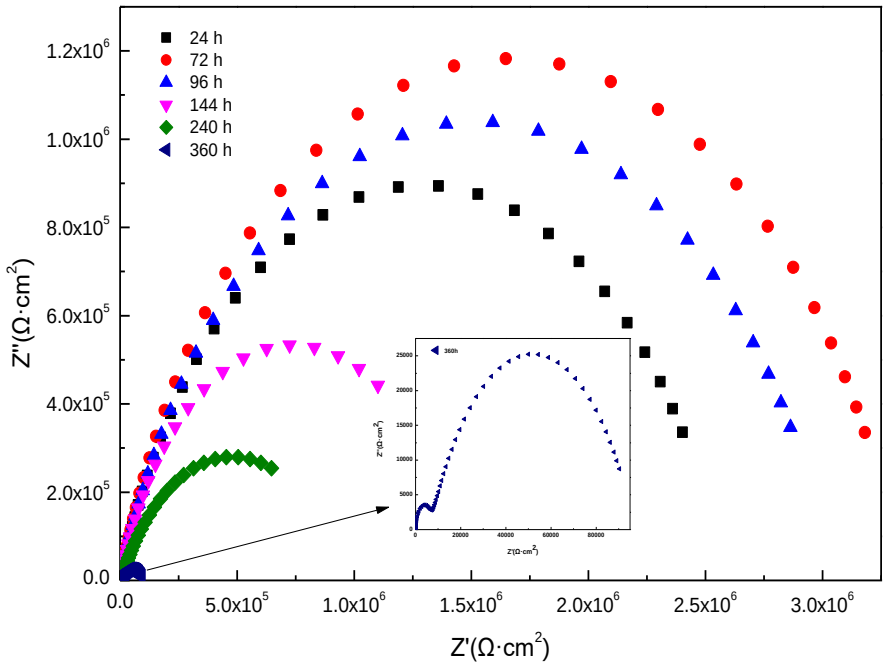

Figure 8. (a) Nyquist plots of AKT-WPU coating after different immersion time in 3.5%NaCl

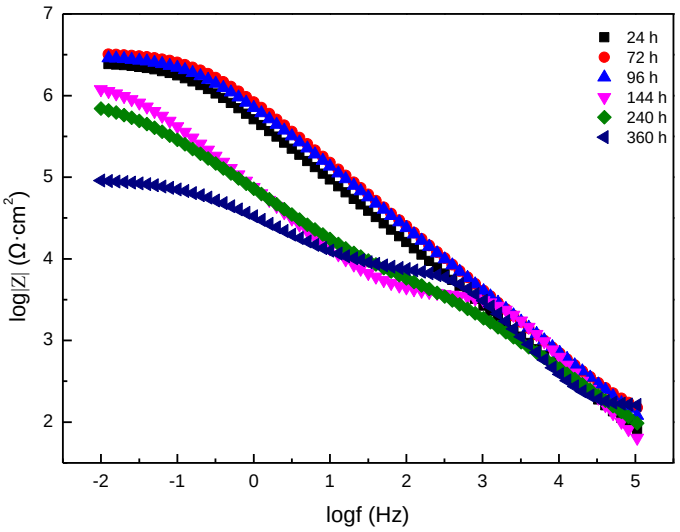

Figure 8. (b) Bode plot of AKT-WPU coating after different immersion time in 3.5%NaCl

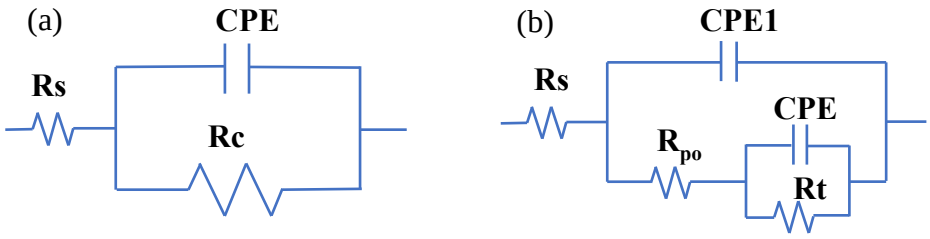

Figure 9. equivalent circuit diagram of AKT-WPU at different soaking stages

Fig. 7 shows that, compared with the pure WPU coating, the coating to which AKT was added completely shifted to the upper left corner, the corrosion potential increased, and the corrosion current density decreased. The parameters of the polarization curve fitted by Cview software are shown in Table 2. With an increase in the amount of AKT added, the corrosion current density of the composite coating decreased first and then increased. The corrosion current density of the coating with a 0.7% AKT addition was at least 5.21×10^{-9} A. The coating with a 1.5% addition had a corrosion current density of up to 2.58×10^{-8} A. This is consistent with our impedance spectrum results. In contrast, the composite coating with AKT added has a corrosion current density less than two orders of magnitude lower than that of a pure WPU coating. Our EIS test proves that the 0.7% AKT coating has a corrosion inhibition efficiency of 99.54% and excellent corrosion resistance.

Table 3. Data of Rs, Rc and Rt for different AKT content coatings by Nyquist plots fitting

Soaking time	Rs (Ω)	CPE1 (F)	Rc (Ω)	CPE2 (F)	Rt (Ω)
24h	22.91	4.32×10^{-7}	2.58×10^{6}	-	-
72h	46.69	2.54×10^{-7}	3.35×10^{6}	-	-
96h	33.62	3.09×10^{-7}	4.06×10^{6}	1.70×10^{-8}	2.57
144h	29.92	2.48×10^{-8}	1.27×10^{4}	2.41×10^{-6}	1.10×10^{6}
240h	35.01	2.78×10^{-6}	4.74×10^{4}	1.10×10^{-6}	8.75×10^{5}
360h	61.15	4.54×10^{-8}	6701	8.75×10^{-6}	9.01×10^{4}

The composite coating with the addition of 0.7% AKT was immersed in a 3.5% NaCl solution for different durations, and the EIS chart was tested as shown in Fig. 8. It can be seen from Fig. 8(a) that as the immersion time increases, the impedance arc of the composite coating first increases and then decreases. The composite coating still has a large impedance arc after 144 h of soaking because the AKT in the coating is evenly distributed, which improves the density of the coating and hinders the transmission of corrosive media[26].

However, the impedance map after 360 h of immersion adds an inconspicuous impedance arc in the high frequency region, indicating that the corrosive medium has reached the surface of the substrate. Fig. 8(b) shows that as the immersion time increases, the log(z)~log(f) curve moves toward the low frequency direction.

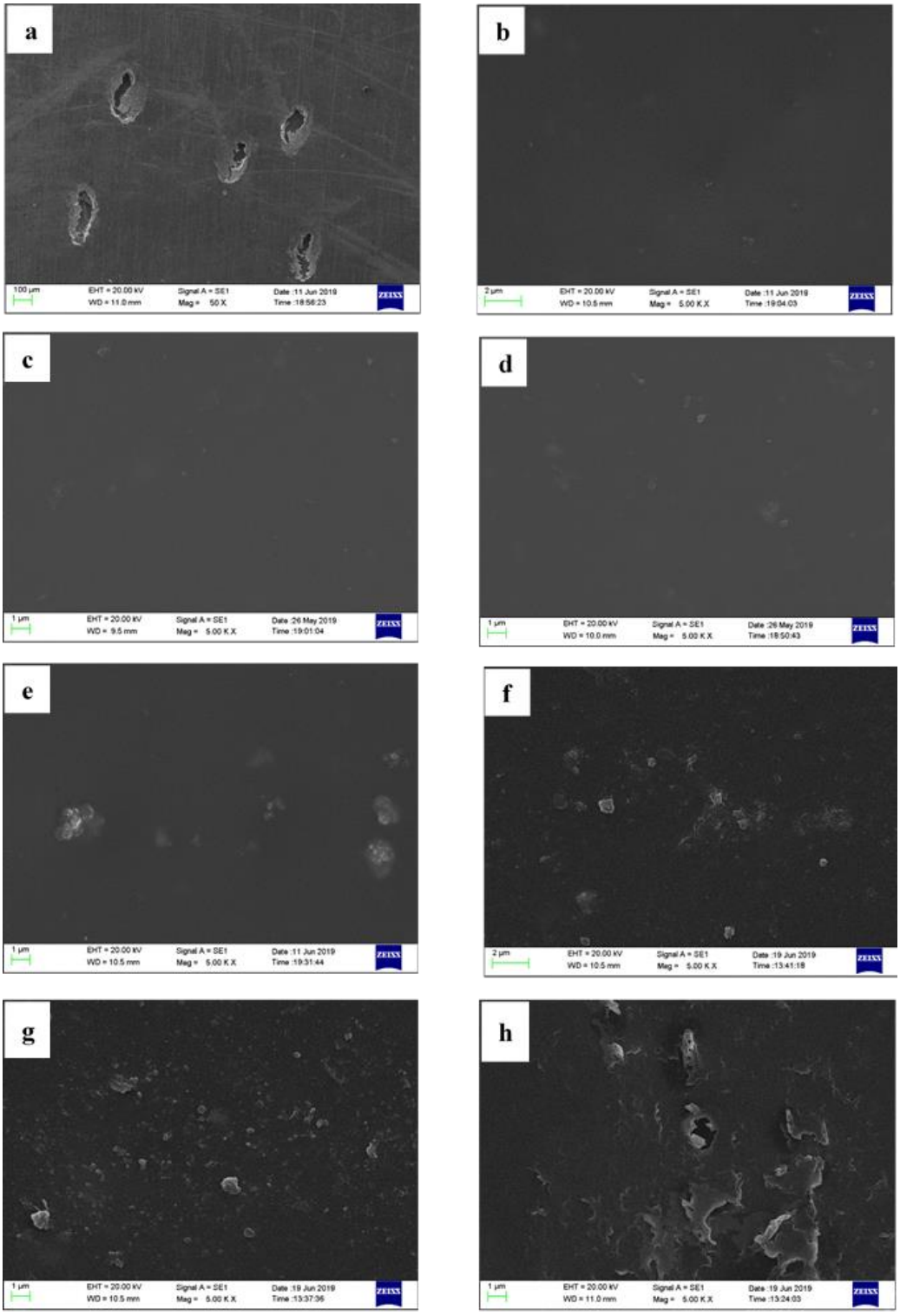

Figure 10. Scanning electron micrograph of AKT-WPU at different soaking stages

In addition, the impedance modulus decreases continuously, indicating that infiltration of the corrosive medium causes the coating resistance to decrease. Fig. 9 is an equivalent circuit diagram for fitting electrochemical impedance data for different soak duration. Fig. 9(a) is an equivalent circuit diagram at the initial stage of immersion, and Fig. 9(b) is an equivalent circuit diagram at the middle stage of immersion. In Fig. 9, Rs, Rc and Rt represent solution resistance, coating resistance and charge transfer resistance, respectively. Table 3 shows the electrochemical impedance parameters of the AKT-WPU coating immersed for different durations. The soaking time increased from 24 h to 72 h, and the coating resistance increased significantly. When the immersion time is 96 h, the coating resistance is slightly reduced, and the charge transfer resistance is small and negligible. When the immersion time reached 144 h, the coating resistance decreased by two orders of magnitude, and the charge transfer resistance increased sharply. This is because the corrosive medium begins to slowly penetrate into the coating. When immersed for 240 h, the coating resistance increases while the charge transfer resistance decreases. This is because the corrosive medium has penetrated into the interior of the coating, decreasing the adhesion of the coating to the substrate[27]. When the immersion time is increased to 360 h, the corrosive medium has completely penetrated into the interior of the coating, a barrier layer is formed between the coating and the substrate, and the metal matrix begins to corrode.

In order to understand the corrosion process of the coating more intuitively, we performed an SEM observation on the surface of the coating which was immersed for different durations as shown in Fig. 10.

Stainless steel (Fig. 10a) forms a significant pitting after being soaked in a 3.5% NaCl solution. Before soaking (Fig. 10b), the surface of the coating is smooth and dense. The surface morphology did not change significantly after soaking for 24 h and 72 h (Fig. 10c and 10d, respectively). This shows that AKT is evenly distributed in the coating, which improves the compactness of the coating and protects the substrate from corrosive media. After immersion for 96 h, a slightly uneven surface appeared on the surface of the coating (Fig. 10e), indicating that a small amount of corrosive medium penetrated the coating. After immersion for 144 h (Fig. 10f) and immersion for 240 h (Fig. 10g), the surface of the coating showed a noticeable irregularity, and a block appeared on the surface of the coating. This is consistent with Liu's[28] observation of the micro-structure of the coating surface by field emission scanning electron microscopy. This indicates that the infiltration of corrosive medium causes the adhesion of the coating to begin to decrease, which also proves that the coating resistance value drops significantly after 144 h of immersion. After soaking for 360 h (Fig. 10h), the surface of the coating formed a massive accumulation and began to appear as corrosion pits, at which time the corrosive medium could easily enter the substrate and corrode.

4. CONCLUSION

Our research findings can be summarized as follows. First, compared with the pure WPU coating, the Water absorption of the AKT-WPU composite coating immersed in 3.5% NaCl for 48 h is stable to 0.473%, and the water resistance of the composite coating is significantly improved. At the same time, the water contact angle of the composite coating also increased from 57.68° to 86.51°. These results

indicate that the AKT particles are uniformly dispersed in the polyurethane coating, which reduces the voids in the composite coating and improves the compactness of the coating to enhance the water resistance of the coating. Second, the EIS and polarization curves show that AKT can improve the corrosion resistance of the coating. When 0.7% AKT is added, the resistance of the AKT-WPU composite coating can reach 5.05×10^{6} Ω, the corrosion current density is 5.21×10^{-9}A, and corrosion inhibition efficiency can reach 99.54%. Third, the SEM image of the AKT-WPU composite coating showed that the surface of the unsoaked composite coating was smooth and compact, and that the surface change of the coating was not obvious at the initial stage of immersion indicating that the coating still has a protective effect after soaking for 360 h. Our research results, as presented in this study, can broaden the scope of application of WPU.

ACKNOWLEDGEMENTS
This work was supported by the National Natural Science Foundation of China (No.51774242)

References

1. Z. Liu, Y. Dong, Z. Chu, Y. Yang, Y. Li and D. Yan, *Mater. Des.*, 52 (2013) 630.
2. A.A. Nazeer and M. Madkour, *J. Mol. Liq*., 253 (2018) 11.
3. M. Ates, *J. Adhes. Sci. Technol.,* 30 (2016) 1510.
4. P.A. Sørensen, S. Kiil, K.D. Johansen and C.E. Weinell, *J. Coat. Technol. Res*., 6 (2009) 135.
5. Z. Ahmad and F. Patel, *Int. J. Corros*., 15 (2011) 396.
6. K.W. Cai, S.X. Zuo, S.P. Luo, C. Yao, W.J. Liu, J.F. Ma, H.H. Mao and Z.Y. Li, *Rsc Adv*., 6 (2016) 95965.
7. J. Sun, H.G. Fang, H.L. Wang, S.Z. Yang, S.R. Xiao and Y.S. Ding, *J. Polym. Eng*., 37 (2017) 113.
8. D.H. Abdeen, E.M. Hachach, M. Koc and M.A. Atieh , *Mater.,* 12 (2019) 210.
9. X.X. Qiao, D.M. Wan and Y.G. Li, *Int. J. Electrochem. Sci.,* 11 (2016) 6023.
10. Z.X. Yu, H.H. Di, Y. Ma, Y. He, L. Liang, L. Lv, X. Ran, Y. Pan and Z. Luo, *Surf. Coat. Technol*., 276 (2015) 471.
11. X.K. Cui, G.Y. Zhu, Y. F. Pan, Q. Shao, C Zhao, M.Y. Dong, Y. Zhang and Z.H. Guo, *Polymer*, 138 (2018) 203.
12. N. Wang, W. Fu, M. Sun, J. Zhang and Q. Fang, *Br. Corros. J.*, 51 (2016) 365.
13. C.X. Wang, H.Y. Mao, C.X. Wang and S.H. Fu, *Ind. Eng. Chem. Res.*, 50 (2011) 11930.
14. Y.F. Zhu, J. Zhang, Y.Y. Zhang, M. Ding, H.Q. Qi, R.G. Du, and C.J. Lin, *Acta Phys.-Chim. Sin.*, 28 (2012) 393.
15. A.N. Murashkevich, O.A. Alisienok, I.M. Zharskii, E.V. Korobko and Z.A. Novikova, *Colloid J.,* 79 (2017) 87.
16. O.D. Lewis, G.W. Critchlow, G.D. Wilcox, A. Dezeeuw, and J. Sander, *Prog. Org. Coat*., 73 (2012) 88.
17. A. Malavika, K. Sasidhar, R.G. Rohit, N. Ramanuj and K.V.S.N. Raju, *J. Polym. Res*., 21 (2014) 600.
18. K.P. Chen, Q. Tian, C.R. Tian, G.Y. Yan, F. Cao, S.E. Liang and X.L. Wang, *Ind. Eng. Chem. Res.*, 56 (2017) 11827.
19. A.V. Rudakova, U.G. Oparicheva, A.E. Grishina, A.A. Murashkina, A.V. Emeline and D.W. Bahnemann, *J. Colloid Interface Sci.,* 466 (2016) 452.
20. A.V. Rudakova, A.V. Emeline and D.W. Bahnemann, *J. Phys. Chem. C,* 14 (2019) 8884.
21. X.T. Wang, S.M. Olsen, A.M. Eduardo, K.N. Olsen and S. Kiil, *J. Coat. Technol. Res*., 15 (2018)

657.
22. N. Marsi and A.Z.M. Rus, *IOP Conf. Ser.: Mater. Sci. Eng.*, 226 (2017) 12161.
23. C.S. Xu, O.Y. Lei, H.Y. Liu, Q.W. Wei, Z.S. Cai, J.W. Xing and Y. Li, *Text. Res. J.*, 85 (2015) 2040
24. F.F. Deng, Y.L. Zhang, X. Li, Y.W. Liu, Z.Q. Shi and Y.H. Wang, *Polym. Compos*., 40 (2018) 328
25. L. Jing, L.Z. Gan, Y.C. Liu, M. Srikanth, W. Lei, Y. Chen and J.H. Yang, *Eur. Polym. J.*, 104 (2018) 57
26. P. Salazar-Bravo, D.D. Angel-López, A.M. Torres-Huerta, M.A. Domínguez-Crespo, D. Palma-Ramírez and A.B. López-Oyama, *Prog. Org. Coat.*, 135 (2019) 51
27. R.H. Patel and P.M. Kapatel, *Int. J. Polym. Anal. Charact.*, 18 (2018) 1548
28. F. Liu and G.D. Liu, *J. Polym. Res.*, 25 (2018) 59